Carbohydrate Polymers 83 (2011) 1665–1671

Contents lists available at ScienceDirect

Carbohydrate Polymers

journal homepage: www.elsevier.com/locate/carbpol

Particulate structure of phytoglycogen nanoparticles probed using amyloglucosidase

Lei Huang [1], Yuan Yao *

The Department of Food Science, Purdue University, 745 Agriculture Mall Drive, West Lafayette, IN 47907, United States

ARTICLE INFO

Article history:
Received 17 August 2010
Received in revised form 7 October 2010
Accepted 11 October 2010
Available online 19 October 2010

Keywords:
Phytoglycogen
Particulate structure
Molecular density
Amyloglucosidase

ABSTRACT

Phytoglycogen is a plant-based, high-density carbohydrate nanoparticle that can be used as a starting material for preparing novel functional nano-constructs. In this study, the particulate structure of phytoglycogen was probed using amyloglucosidase hydrolysis, with amylopectin of waxy corn starch as a reference. Glucose release was monitored; molar mass, root mean square (RMS) radius, and dispersed molecular density were evaluated using multiangle laser-light scattering. The goal was to reveal the structural features of phytoglycogen nanoparticles. After extended amyloglucosidase hydrolysis, the total glucose release of phytoglycogen was lower than that of amylopectin. At the initial stage of hydrolysis, however, glucose was released at a higher rate from phytoglycogen, suggesting a dense distribution of nonreducing ends at the surfaces of nanoparticles. The reduction of molar mass and RMS radius caused by amyloglucosidase hydrolysis were much lower for phytoglycogen than for amylopectin. The dispersed molecular density of amylopectin remained at about 60 g/mol nm^3 during hydrolysis. In contrast, the density of phytoglycogen decreased from about 1200 to 950 g/mol nm^3, suggesting a density increment towards the external region of nanoparticle.

1. Introduction

Both starch and phytoglycogen are plant-based carbohydrate polymers that play major roles in energy storage. Due to the importance of starch in the food industry and other areas, amylopectin, a primary component of starch, has undergone substantial structural characterization (Gallant, Bouchet, & Baldwin, 1997; Manners, 1991; Thompson, 2000). In contrast, there have been only a limited number of reports on the structure of phytoglycogen (Wong et al., 2003; Yun & Matheson, 1993). Recently, it was found that glycogen and phytoglycogen can be used as novel templates for synthesizing functional nano-constructs (Putaux, Potocki-Veronese, Remaud-Simeon, & Buleon, 2006; Scheffler, Wang, Huang, San-Martin Gonzalez, & Yao, 2010a, Scheffler, Huang, Bi, & Yao, 2010b). For example, phytoglycogen can be used to prepare phytoglycogen octenyl succinate, an amphiphilic carbohydrate nanoparticle, to substantially improve lipid oxidative stability of emulsions (Scheffler et al., 2010a). These studies highlight the importance of carbohydrate nanoparticles in designing novel biomaterials.

The largest source of phytoglycogen is the kernel of the maize mutant *sugary-1* (*su1*) (Morris & Morris, 1939), a major genotype of sweet corn. Phytoglycogen has also been found in mutant sorghum (Boyer & Liu, 1983), rice (Nakamura, Umemoto, Takahata, Komae, & Amano, 1996; Wong et al., 2003), barley (Burton et al., 2002), and *Arabidopsis* (Zeeman et al., 1998). In maize, the *su1* mutation leads to a deficiency of SU1, an isoamylase-type starch-debranching enzyme (DBE) (James, Robertson, & Myers, 1995). In DBE deficiency, the highly branched phytoglycogen is formed, replacing starch granules. Phytoglycogen particle size usually ranges from 30 to 100 nm (Putaux, Buleon, Borsali, & Chanzy, 1999). The highly branched structure of phytoglycogen results in its unusually high molecular density in aqueous dispersion. In rice, the dispersed molecular density of phytoglycogen is over 10 times that of starch (Wong et al., 2003). The dispersed molecular density of phytoglycogen from maize is over 1000 g/mol nm^3 compared to approximately 40 g/mol nm^3 for amylopectin (Scheffler et al., 2010a). In phytoglycogen molecules, there are no long chains connecting individual clusters, an essential feature of amylopectin molecules (Shin, Simsek, Reuhs, & Yao, 2008; Thompson, 2000). The average chain length of phytoglycogen ranges from DP (degree of polymerization) 11–12 and branch density (i.e., the percentage of α-1,6 glucosidic linkages) is about 8–9%. In contrast, the average chain length and branch density of amylopectin are DP17-18 and 6%, respectively (Shin et al., 2008; Yun & Matheson, 1993).

In the current study, amyloglucosidase (EC 3.2.1.3) was used to probe the structure of phytoglycogen nanoparticles, using amylopectin from waxy corn starch as a reference. Amyloglucosidase

* Corresponding author. Tel.: +1 765 494 6317; fax: +1 765 494 7953.
E-mail address: yao1@purdue.edu (Y. Yao).
[1] Visiting student from Harbin University of Commerce, China.

0144-8617/$ – see front matter © 2010 Elsevier Ltd. All rights reserved.
doi:10.1016/j.carbpol.2010.10.030

is an exo-acting enzyme that hydrolyzes both α-1,4 and α-1,6 glucosidic linkages from the nonreducing ends to yield glucose (Hizukuri, 1996). Amyloglucosidase hydrolyzes α-1,6 linkages at a rate about 1/30 of that for α-1,4 linkages (Pazur & Kleppe, 1962), and it does not proceed through a branch point unless the α-1,6 linkage is removed (Hizukuri, 1996). Such a hydrolysis pattern can realize an "outside-in" trimming of glucan molecules. By monitoring glucose release and the structure of residual phytoglycogen and amylopectin molecules, information was obtained on the particulate structures of these glucan molecules, and in particular, the phytoglycogen nanoparticles.

2. Materials and methods

2.1. Materials

Waxy corn starch was obtained from the National Starch Food Innovation (Bridgewater, NJ). Mature kernels of the sweet corn "Silver Queen" *sugary* (*su1*) line were purchased from Burpee Co. (Warminster, PA). Amyloglucosidase from *Aspergillus niger* was purchased from Megazyme Co. (Wicklow, Ireland).

2.2. Methods

2.2.1. Extraction of phytoglycogen

To extract phytoglycogen, 320 g of dry kernels were coarsely ground and soaked in ten times their weight of precooled deionized water for 4 h at 4 °C. The suspension was homogenized using a high-speed blender (Waring Laboratory). The homogenates were collected and passed through a 270-mesh sieve, and the solid was further extracted twice using deionized water. Thereafter, the combined liquid was adjusted to pH 4.9 with acetic acid and placed at 4 °C for 2 h to induce protein precipitation. The liquid was then centrifuged at 10,000 × *g* at 4 °C and the creamy layer and precipitate were removed. The supernatant was adjusted to pH 7.0 and autoclaved at 121 °C for 20 min. The denatured, insoluble proteinaceous materials were removed by centrifugation. To the collected supernatant, three volumes of ethanol were added to precipitate polysaccharides. The precipitate was washed with three cycles of ethanol dispersion-centrifugation. After removing the bulk of ethanol by filtration, the solid material was placed in a fume hood to remove residual ethanol. The collected powder material (around 110 g) was the phytoglycogen material used in this study.

2.2.2. Preparation of non-granular waxy corn starch (WCS)

To disperse WCS granules, 60 g of starch was suspended in 20 times its weight of a 90% DMSO solution. The suspension was stirred in a boiling-water bath until the liquid became clear and then homogenized using a high-speed blender. The liquid was added to three volumes of ethanol to precipitate the polysaccharide. The precipitate was washed with three cycles of ethanol dispersion-centrifugation. After removing the bulk of ethanol by filtration, the solid material was placed in a fume hood to remove residual ethanol. The collected powder was the non-granular WCS material used in this study.

2.2.3. Transmission electron microscopy (TEM)

TEM imaging was conducted as described by Scheffler et al. (2010b).

2.2.4. Amyloglucosidase treatment of phytoglycogen and WCS

To fully disperse phytoglycogen and non-granular WCS in the buffer without causing lumps, each glucan solid (in the powder form) and required amount of buffer were divided into multiple portions and then mixed in a portion-by-portion procedure. Right after each mixing, vortex was applied to ensure a complete suspension. In this way, 20 mL each of 0.50%, 2.0%, or 4.0% phytoglycogen or WCS dispersions in 50 mM sodium acetate buffer (pH 4.5) were prepared. Each preparation was then prewarmed at 40 °C for 10 min. Amyloglucosidase 20 units (in 20 μL) was added to each dispersion, giving enzyme activity/glucan ratios of 200, 50, and 25 U/g. Aliquots were withdrawn from each test reaction at 0.5, 1, 2, 3, 5, 10, 20, 30, 60, 120, 240, 480, and 960 min. The reaction in each aliquot was terminated by adding an equal volume of 4.0% sodium hydroxide. The amount of glucose in each aliquot was determined using the Nelson-Somogyi assay (Somogyi, 1952) standardized using glucose. The standard glucose oxidase/peroxidase method was not used due to the low concentration of glucose at the initial stage of amyloglucosidase hydrolysis.

2.2.5. Determination of weight-average molar mass, Z-average root mean square (RMS) radius, and dispersed molecular density

Another set of amyloglucosidase treatments of phytoglycogen and WCS was conducted with the same protocol as described above, using 20 mL of 4.0% phytoglycogen or WCS dispersion with 20 units of amyloglucosidase added. Aliquots were withdrawn at 5, 10, 20, 30, 60, 120, 240, and 480 min and heated in a boiling-water bath for 10 min. Each sample was subjected to high-performance size-exclusion chromatography (HPSEC) consisting of an isocratic pump (515 HPLC, Waters), an injector (Model 7725i with a 20-μL sample loop, Rheodyne), a multiangle laser-light scattering detector (MALLS, Dawn HELEOS-II, Wyatt Technology) with a He–Ne Laser source (λ = 632.8 nm), and a refractive-index detector (RI, OptilabrEX, Wyatt Technology). Two connected columns (PL Aquagel-OH 40 15 μm and 60 15 μm, Polymer Laboratories, Varian) with a guard column were used for separation using deionized water (pH 6.8, containing 0.02% sodium azide) as the mobile phase at a flow rate of 1.0 mL/min. Astra software (Version 5.3.4.14, Wyatt Technology) was used to determine molar mass and RMS radius. Curve fitting to calculate both molar mass and RMS radius at each elution point was based on a first-order Berry model in which the second virial coefficient A_2 was set to zero. The dn/dc value of 0.146 was used for calculations. For individual peaks identified in the chromatograms, the weight-average molar mass (M_W, g/mol) and Z-average RMS radius (R_Z, nm) were obtained using the Astra software. Dispersed molecular density (ρ, g/mol nm^3) was calculated as $\rho = M_W/R_Z^3$ (Wong et al., 2003). For each glucan material, three injections were made and the mean values of M_W, R_Z, and ρ were obtained along with the standard deviations.

The recommended flow rate of both columns (PL Aquagel-OH 40 15 μm and PL Aquagel-OH 60 15 μm) was 1.0 mL/min. To evaluate the impact of flow rate on potential shear degradation of polysaccharides in columns (Gidley et al., 2010), both phytoglycogen and WCS were later tested again using flow rates of 0.5 and 1.0 mL/min. In addition, pullulan standards with M_W of 1.12×10^5 and 2.12×10^5 g/mol were tested with both flow rates. This effort allowed us to evaluate the quality of HPSEC-MALLS-RI analysis.

3. Results and discussion

3.1. TEM imaging of phytoglycogen nanoparticles

As shown in Fig. 1, most phytoglycogen nanoparticles had a spherical shape with diameters around 40–50 nm. This particle-size range differs slightly from the range of 30–100 nm reported by Putaux et al. (1999). In our procedure, an autoclave was used to remove proteinaceous materials, which simultaneously removed a portion of the phytoglycogen aggregates and thus likely reduced the particle size of the isolated phytoglycogen. In comparison, amylopectin molecules usually have a well-dispersed,

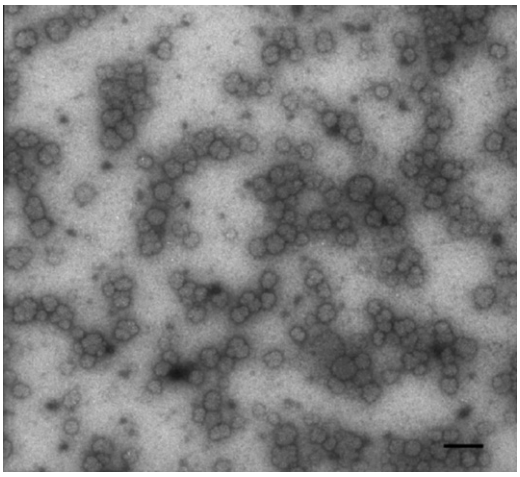

Fig. 1. Transmission electron microscope image of phytoglycogen nanoparticles (scale bar: 100 nm).

wormlike conformation as described by Putaux, Buleon, and Chanzy (2000).

3.2. Glucose release from phytoglycogen and WCS

Fig. 2A-1, B-1, and C-1 shows the initial stages of glucose release from phytoglycogen and WCS by amyloglucosidase hydrolysis with enzyme activity/glucan ratios of 200, 50, and 25 U/g, respectively. At the ratio of 200 U/g, the rate of glucose release of phytoglycogen was essentially the same as that of WCS. However, a reduction of the enzyme activity/glucan ratio to 50 U/g led to a slightly higher rate of glucose release from phytoglycogen than from WCS. When the ratio was reduced to 25 U/g, glucose was released at a much higher rate from phytoglycogen than from WCS.

Fig. 2A-2, B-2, and C-2 shows the glucose-release profiles over the 960-min reaction period. In general, the overall glucose release from phytoglycogen was lower than that from WCS regardless of the enzyme activity/glucan ratio. Specifically, the difference in glucose release between phytoglycogen and WCS was larger for the activity/glucan ratio of 25 U/g than for the ratios of 200 or

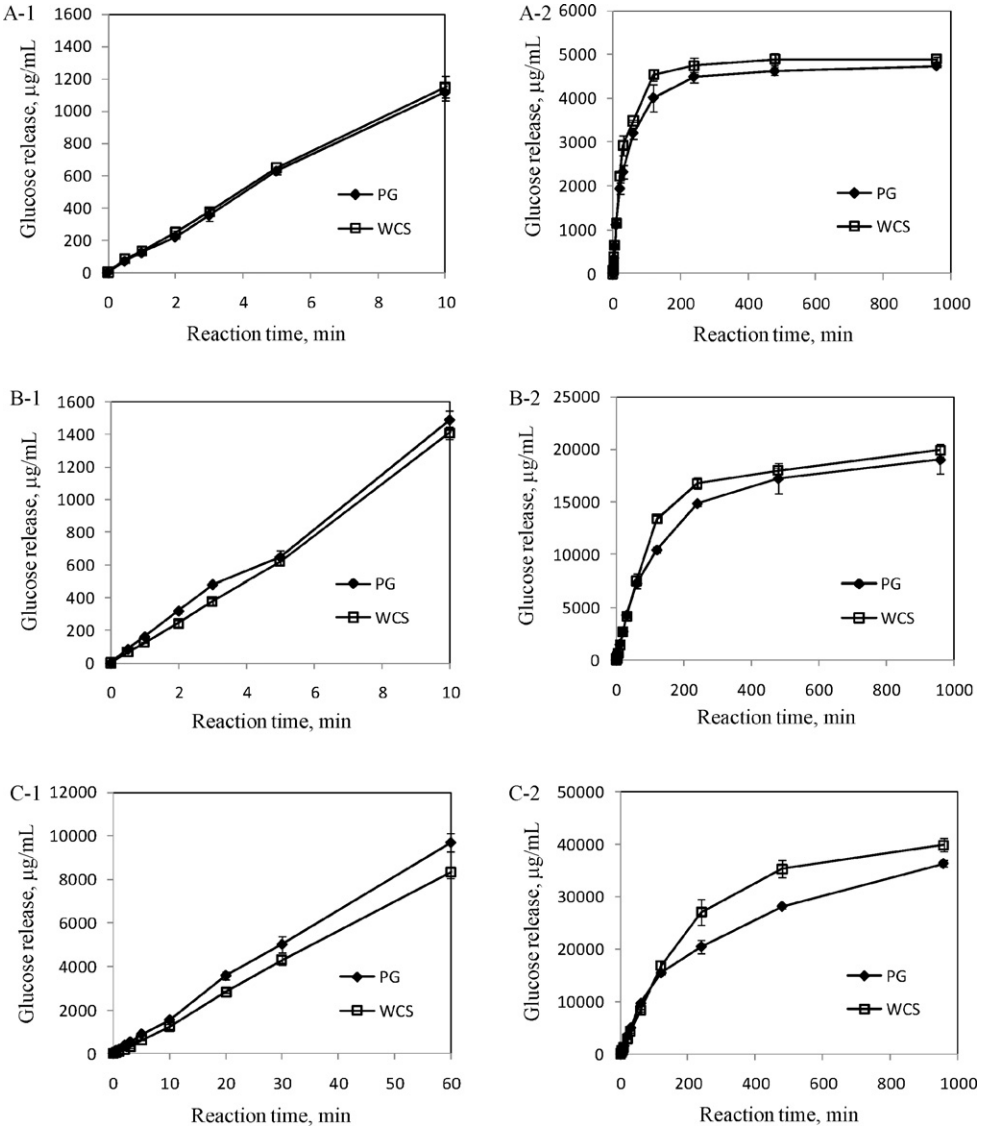

Fig. 2. Initial (A-1, B-1, and C-1) and overall (A-2, B-2, and C-2) glucose-release profiles of phytoglycogen (PG) and waxy corn starch (WCS) subjected to amyloglucosidase hydrolysis. The enzyme activity/glucan ratios for group A, B, and C were 200, 50, and 25 U/g, respectively. Data points are means of three replicates with error bars of standard deviation.

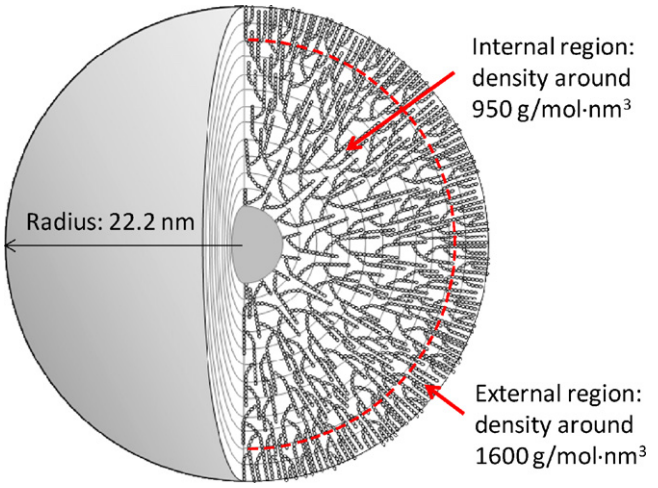

Fig. 3. A highly schematic depiction of an average phytoglycogen nanoparticle. The radius of the nanoparticle and the dispersed molecular density (ρ) of the internal and external regions are indicated. The thickness of the external region is about 3.3 nm.

50 U/g. Glucose release reached a plateau after 240 min for 200 U/g, whereas for 25 U/g there was still a potential for glucose release even after 960 min.

Associated with the interaction between amyloglucosidase and α-glucans, the rate of glucose release is governed by: (1) the amount and concentration of nonreducing ends accessible to enzyme molecules, (2) the enzyme concentration, and (3) the abundance of α-1,6 glucosidic linkages. Among these factors, the second was the same for phytoglycogen and WCS, and the first and third factors were affected by the structures of phytoglycogen and amylopectin of WCS.

As depicted in Fig. 3, a phytoglycogen nanoparticle is believed to have short linear chains densely distributed at the surface. In contrast, for the dispersed amylopectin molecules of WCS, the side chains are highly flexible due to the presence of intercluster chains. At the initial stage of amyloglucosidase hydrolysis, effective binding occurred between enzyme molecules and nonreducing ends. For amylopectin, due to its low molecular density and conformational flexibility, most, if not all, nonreducing ends were probably accessible to the enzyme. In contrast, for phytoglycogen nanoparticles only the nonreducing ends at the outer surface were accessible to the enzyme. However, the local concentration of nonreducing ends at the surface of phytoglycogen nanoparticles could be much higher than that of amylopectin. With an excess of enzyme (200 U/g), the low accessibility of nonreducing ends inside phytoglycogen nanoparticles was compensated for by the high local concentration of nonreducing ends at surface, leading to a rate of glucose release comparable to that of amylopectin of WCS. With reduced enzyme dose (25 U/g), the accessibility of nonreducing ends to enzyme molecules was no longer a major factor, and the high density of nonreducing ends at the surface of nanoparticles led to the higher rate of glucose release from phytoglycogen than from WCS.

As amyloglucosidase hydrolysis proceeded, the outer layer of linear chains was removed and α-1,6 glucosidic linkages were exposed. Because the reaction rate of amyloglucosidase with α-1,6 linkages is about 1/30 of that of α-1,4 linkages (Pazur & Kleppe, 1962), the presence of branches substantially reduced the rate of glucose release. For phytoglycogen, the branch density is around 9% (Shin et al., 2008; Yun & Matheson, 1993), much higher than that of amylopectin of WCS (6%). Therefore, glucose release from phytoglycogen was lower than that from WCS over an extended period of hydrolysis regardless of the enzyme activity/glucan ratio.

3.3. M_W and R_Z of phytoglycogen and WCS

Fig. 4A and B shows the definition of pure phytoglycogen, intermediate materials, and amylopectin in the HPSEC chromatograms. To determine the fitting model for calculating M_W and R_Z, we selected the data slice at the peak position of pure phytoglycogen and amylopectin. Two models, first- and second-order Berry were compared. Their plots are indicated in Fig. 4C and D. In general, the fitting quality appears similar between the first- and second-Berry models. To evaluate the effect of models on the average data (i.e. M_W and R_Z) of defined materials, the calculated numbers and their so-called "uncertainties" were compared among four models, i.e. first- and second-Berry and first- and second-order Zimm (data not shown). The uncertainties of exported data are ASTRA software-calculated values that incorporate factors including the Chi-squared values returned from the fit; therefore, they can be used to evaluate the quality of fitting. For amylopectin, all four models gave essentially the same results for M_W. However, a first-order Zimm gave abnormally high value of R_Z. The uncertainties of both M_W and R_Z were the lowest for a first-order Berry fitting. For phytoglycogen, all four models gave essentially the same result for M_W. However, a second-order Zimm gave abnormally low value of R_Z. The uncertainties of both M_W and R_Z were the lowest for a first-order Berry and first-order Zimm. Therefore, we selected the first-order Berry fitting for phytoglycogen, amylopectin, and their residues after enzymatic treatments.

As shown in Table 1, the impact of flow rate, 0.5 and 1.0 mL/min on the measured M_W and R_Z of pure phytoglycogen and amylopectin was almost negligible. In addition, the measured M_W of two pullulan standards was reasonably consistent with the specifics of products at flow rates of 0.5 and 1.0 mL/min. The columns used consisted of two high-performance size-exclusion columns with particle size of 15 μm. Such a large particle size of stationary phase may substantially reduce the potential of shear degradation of polysaccharides during separation.

Fig. 5 shows the HPSEC-MALLS-RI chromatograms of phytoglycogen and WCS subjected to amyloglucosidase hydrolysis. For native phytoglycogen and its macromolecular residues, a major (left) and minor population (right) can be identified. The two populations bordered at the retention time of 15.5 min. In this study, the major population was defined as "pure phytoglycogen", and the minor population as "intermediate material". For native WCS, there was only one population that was amylopectin.

Fig. 6A shows the impact of amyloglucosidase hydrolysis on the M_W of pure phytoglycogen, intermediate material, and WCS. Without amyloglucosidase hydrolysis, the M_W of pure phytoglycogen, intermediate material, and WCS were 1.30, 0.48, and 4.00×10^7 g/mol, respectively. During amyloglucosidase hydrolysis, the M_W of WCS decreased rapidly and reached 0.16×10^7 g/mol after 120 min. In contrast, the M_W reductions of pure phytoglycogen and intermediate material were much slower, reaching 0.83 and 0.27×10^7 g/mol, respectively, after 120 min. After 480 min of hydrolysis, the M_W values of pure phytoglycogen and intermediate material were reduced to 0.44 and 0.14×10^7 g/mol, respectively.

Fig. 6B shows the impact of amyloglucosidase hydrolysis on the R_Z of pure phytoglycogen, intermediate material, and WCS. The pattern of R_Z changes was similar to that of M_W. Without amyloglucosidase hydrolysis, the R_Z of pure phytoglycogen, intermediate material, and WCS were 22.2, 21.6, and 86.8 nm, respectively. Apparently, the dispersed amylopectin molecules in WCS were much larger in size than pure phytoglycogen and intermediate material. During amyloglucosidase hydrolysis, the R_Z of amylopectin in WCS decreased rapidly, reaching 33.0 nm after 120 min. In contrast, R_Z decreased much more slowly for pure phytoglycogen and intermediate material, reaching 20.0 and 16.9 nm, respectively, after 120 min.

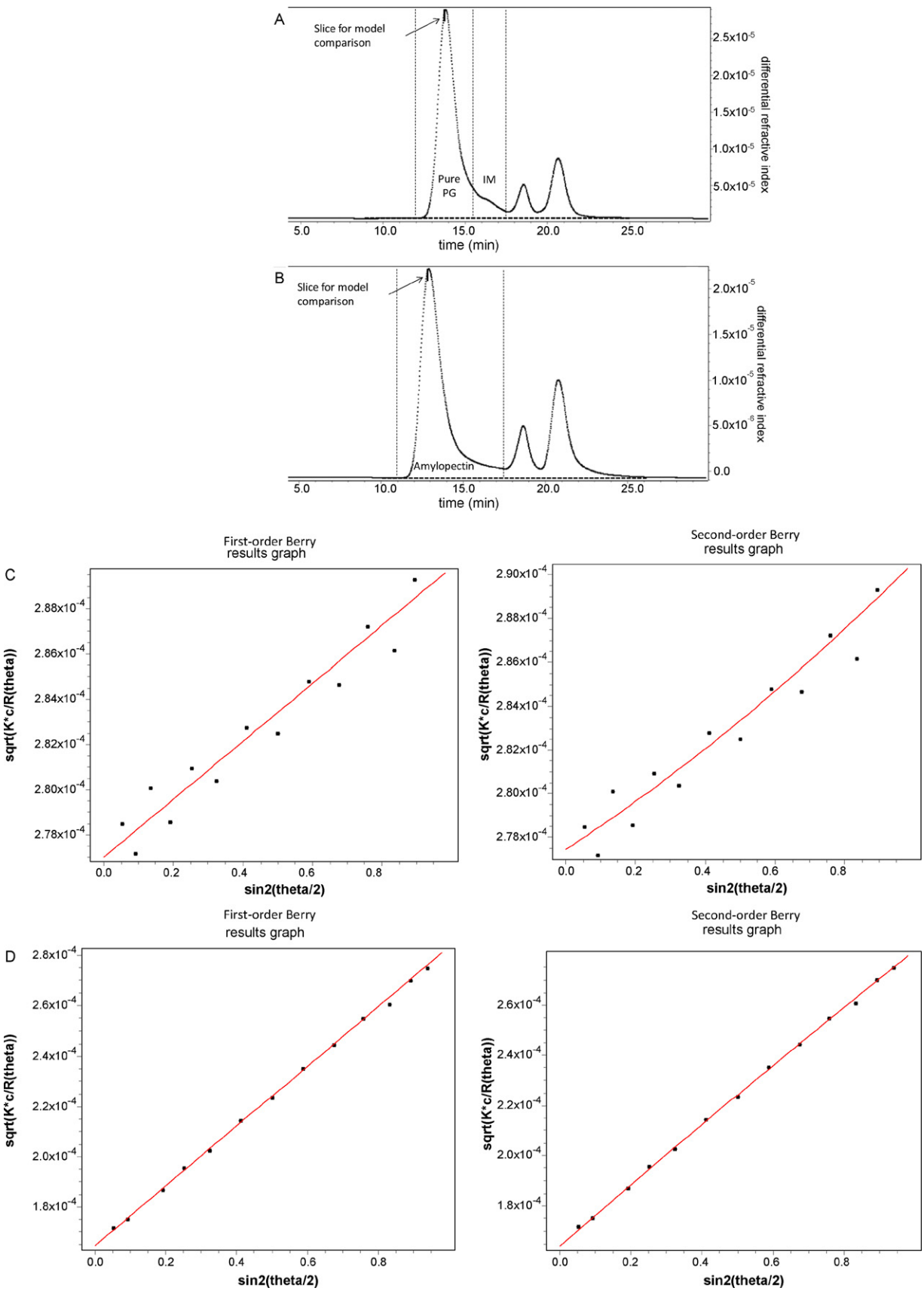

Fig. 4. HPSEC chromatograms of phytoglycogen (A) and waxy corn starch (B), and the first- and second-order Berry plots of the chromatogram slices for phytoglycogen (C) and amylopectin (D). Definitions of pure phytoglycogen (pure PG), intermediate materials (IM), and amylopectin are indicated. Also indicated are the chromatogram slices of phytoglycogen and amylopectin used for comparing the first- and second-order Berry plots. The scale of *Y*-axis for amylopectin Berry plots is 10 times that for phytoglycogen, leading to seemingly more scattered points for phytoglycogen plots.

Table 1
Calculated weight-average molar mass (M_W) and *Z*-average root mean square radius (R_Z) of pure phytoglycogen and amylopectin, and M_W of two pullulan standards at different mobile phase flow rates of size-exclusion chromatography.

	M_W (g/mol)		R_Z (nm)	
	Flow rate 0.5 mL/min	Flow rate 1.0 mL/min	Flow rate 0.5 mL/min	Flow rate 1.0 mL/min
Phytoglycogen	1.306×10^7	1.305×10^7	22.4	22.2
Amylopectin	4.184×10^7	4.178×10^7	88.1	86.8
Pullulan, M_W 1.12×10^5 g/mol	1.26×10^5	1.24×10^5		
Pullulan, M_W 2.12×10^5 g/mol	2.09×10^5	2.12×10^5		

3.4. Dispersed molecular density (ρ) of phytoglycogen and WCS

Fig. 6C shows the impact of amyloglucosidase hydrolysis on the ρ values of pure phytoglycogen, intermediate material, and WCS. Without amyloglucosidase hydrolysis, the ρ values of pure phytoglycogen, intermediate material and WCS were 1198, 475, and 62 g/mol nm^3, respectively. Both pure phytoglycogen and intermediate material were much denser than WCS in aqueous dispersion. It is interesting that intermediate material had a ρ value ranging between those of pure phytoglycogen and WCS. During amyloglucosidase hydrolysis, the ρ value of phytoglycogen remained at approximately 1200 g/mol nm^3 for the first 60 min, decreased to 1042 g/mol nm^3 by 120 min, and stabilized at about 950 g/mol nm^3 after 240 min. During this process, the R_Z of pure phytoglycogen deceased from 22.2 to 20.3 nm after 60 min, to 20.0 nm after 120 min, and to 18.9 nm after 240 min.

For an average phytoglycogen nanoparticle, if R_Z is used as an approximate value of the actual radius, it is possible to estimate the molecular density at different radial positions. Assuming phytoglycogen nanoparticle is spherical, the density of a layer of external region (ρ_{ER}) can be calculated as: $\rho_{ER} = (\rho_{native} \times R^3_{native} - \rho_{residue} \times R^3_{residue})/(R^3_{native} - R^3_{residue})$. In this equation, ρ_{native} (1198 g/mol nm^3) and $\rho_{residue}$ are the density of an average native phytoglycogen nanoparticle and

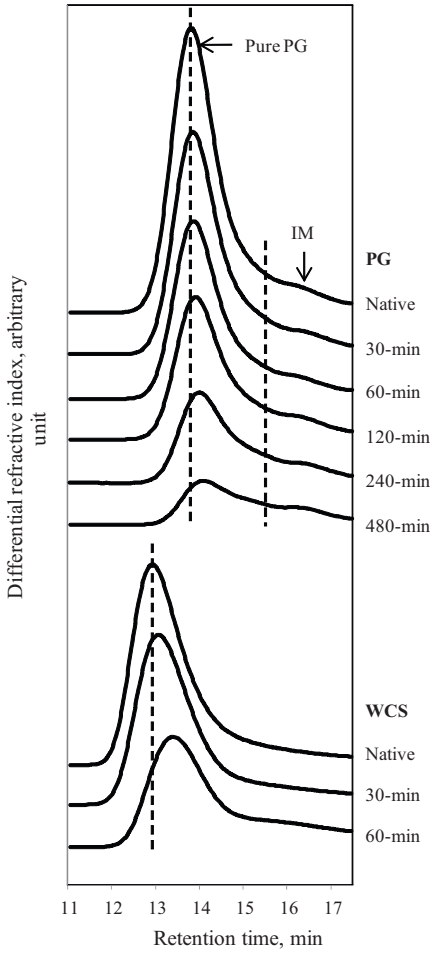

Fig. 5. HPSEC-MALLS-RI chromatograms of phytoglycogen (PG) and waxy corn starch (WCS) subjected to amyloglucosidase hydrolysis for various periods of time. Pure PG and intermediate material (IM) populations are separated by the retention time of 15.5 min (indicated by a dotted line). Dotted lines are also used to indicate the modal positions of pure PG and amylopectin peaks.

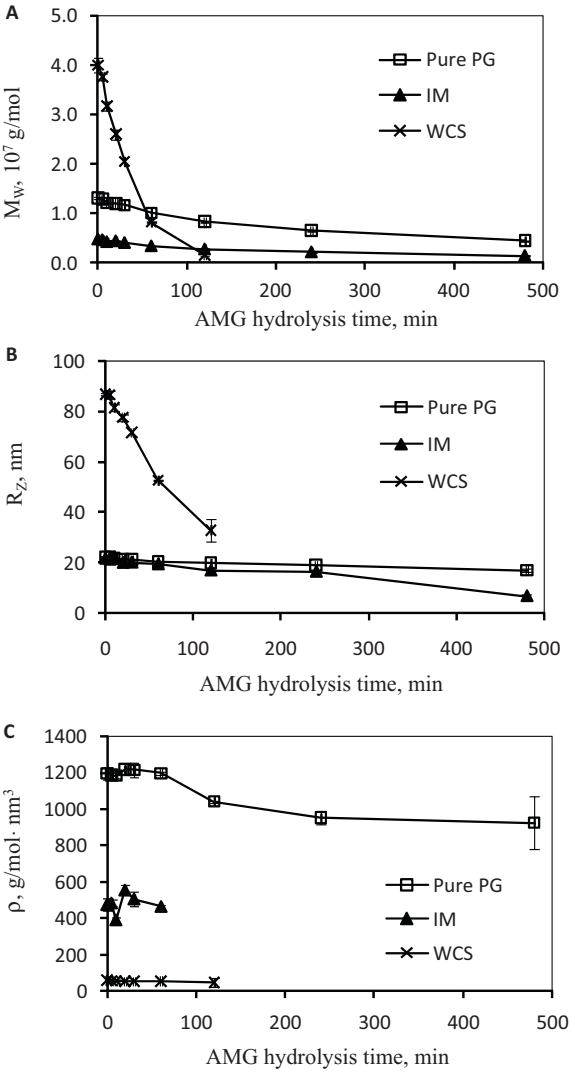

Fig. 6. Weight-average molecular mass (M_W) (A), root mean square radii (R_Z) (B), and dispersed molecular density (ρ) (C) of pure phytoglycogen (pure PG), intermediate material (IM), and WCS subjected to various time periods of amyloglucosidase (AMG) hydrolysis. Data points are means of three replicates with error bars of standard deviation.

Table 2
Effect of generation numbers on the molecular weight (M_W), hydrodynamic diameter (D_H), and dispersed molecular density (ρ) of [cystamine core]-PAMAM dendrimers. Data are adapted from Tomalia (2005). The value of ρ is calculated as $\rho = M_W/(D_H/2)^3$.

Generation	M_W (g/mol)	D_H (nm)	ρ (g/mol nm^3)
2	3348	2.9	1098
3	7001	3.6	1200
4	14,307	4.5	1256
5	28,918	5.4	1469
6	58,140	6.7	1546
7	116,585	8.1	1755

its residue after amyloglucosidase hydrolysis, respectively. R_{native} (22.2 nm) and $R_{residue}$ are the radii of the PG nanoparticle and its residue. After 120 min of amyloglucosidase hydrolysis, $\rho_{residue}$ was 1042 g/mol nm^3 and $R_{residue}$ was 20.0 nm. The calculated ρ_{ER} is then 1622 g/mol nm^3 for an external region with a thickness of 2.2 nm (i.e., 22.2–20.0 nm). After 240 min of amyloglucosidase hydrolysis, $\rho_{residue}$ was 953 g/mol nm^3 and $R_{residue}$ was 18.9 nm. The calculated ρ_{ER} is 1593 g/mol nm^3 for an external region with a thickness of 3.3 nm (i.e., 22.2–18.9 nm). The densities thus calculated for the internal and external regions are indicated in Fig. 3.

For phytoglycogen, the increase of molecular density with the growth of nanoparticles shares a similar pattern with the synthesis of dendrimers. Table 2 lists the calculated ρ values of polyamidoamine (PAMAM) dendrimers based on the data from a review by Tomalia (2005). With synthesis proceeding from generations 2 to 7, the ρ value of the dendrimers increased from 1098 to 1755 g/mol nm^3. For a dendrimer molecule, the steady increase of density with generation number is due to the crowding effect among tethered chains. Based on the same notion, an increased density towards the surfaces of phytoglycogen nanoparticles is associated with the rapid propagation of branches.

In summary, in this work amyloglucosidase was used as a probe to study the particulate structure of phytoglycogen nanoparticles using amylopectin in WCS as a reference. The data supported the assumption that the surfaces of the phytoglycogen nanoparticles are densely covered with linear glucan segments. More importantly, the presence of a density gradient in the nanoparticles was revealed, not only providing information for studying phytoglycogen biosynthesis but also showing the potential for using phytoglycogen nanoparticles as delivery devices. For example, the internal space of the nanoparticles can possibly be used to load bioactive compounds, with the external region as a mechanism for controlled release, either by its inherent high density or by additional surface modifications.

Role of the funding source

A grant from the National Institute of Food and Agriculture of the United States Department of Agriculture supports the experiment design, manuscript writing, sponsorship of the visiting student (Lei Huang), and part of supplies. A grant from the National Science Foundation supports part of supplies. A Purdue Gift fund (to Dr. Yao) supports manuscript editing.

References

Boyer, C. D., & Liu, K. C. (1983). Starch and water-soluble polysaccharides from sugary endosperm of sorghum. *Phytochemistry*, *22*, 2513–2515.
Burton, R. A., Jenner, H., Carrangis, L., Fahy, B., Fincher, G. B., Hylton, C., et al. (2002). Starch granule initiation and growth are altered in barley mutants that lack isoamylase activity. *Plant Journal*, *31*, 97–112.
Gallant, D. J., Bouchet, B., & Baldwin, P. M. (1997). Microscopy of starch: Evidence of a new level of granule organization. *Carbohydrate Polymers*, *32*, 177–191.
Gidley, M. J., Hanashiro, I., Hani, N. M., Hill, S. E., Huber, A., Jane, J., et al. (2010). Reliable measurements of the size distributions of starch molecules in solution: Current dilemmas and recommendations. *Carbohydrate Polymers*, *79*, 255–261.
Hizukuri, S. (1996). Starch: Analytical aspects. In A. C. Eliasson (Ed.), *Carbohydrates in food*. Marcal-Dekker.
James, M., Robertson, D., & Myers, A. (1995). Characterization of the maize gene sugary1, a determinant of starch composition in kernels. *Plant Cell*, *7*, 417–429.
Manners, D. J. (1991). Recent developments in our understanding of glycogen structure. *Carbohydrate Polymers*, *16*, 37–82.
Morris, D. L., & Morris, C. T. (1939). Glycogen in the seed of Zea mays (variety golden bantam). *Journal of Biological Chemistry*, *130*, 535–544.
Nakamura, Y., Umemoto, T., Takahata, Y., Komae, K., & Amano, E. (1996). Changes in structure of starch and enzyme activities affected by sugary mutations in developing rice endosperm. Possible role of starch debranching enzyme (R-enzyme) in amylopectin biosynthesis. *Physiologia Plantarum*, *97*, 491–498.
Pazur, J. H., & Kleppe, K. (1962). Hydrolysis of alpha-D-glucosidides by amyloglucosidase from *Aspergillus niger*. *Journal of Biological Chemistry*, *237*, 1002–1006.
Putaux, J., Buleon, A., Borsali, R., & Chanzy, H. (1999). Ultrastructural aspects of phytoglycogen from cryo-transmission electron microscopy and quasi-elastic light scattering data. *International Journal of Biological Macromolecules*, *26*, 145–150.
Putaux, J., Buleon, A., & Chanzy, H. (2000). Network formation in dilute amylose and amylopectin studied by TEM. *Macromolecules*, *33*, 6416–6422.
Putaux, J. L., Potocki-Veronese, G., Remaud-Simeon, M., & Buleon, A. (2006). Alpha-D-glucan-based dendritic nanoparticles prepared by in vitro enzymatic chain extension of glycogen. *Biomacromolecule*, *7*, 1720–1728.
Scheffler, S. L., Wang, X., Huang, L., San-Martin Gonzalez, F., & Yao, Y. (2010). Phytoglycogen octenyl succinate, an amphiphilic carbohydrate nanoparticle, and ε-polylysine to improve lipid oxidative stability of emulsions. *Journal of Agricultural and Food Chemistry*, *58*, 660–667.
Scheffler, S. L., Huang, L., Bi, L., & Yao, Y. (2010). In vitro digestibility and emulsification properties of phytoglycogen octenyl succinate. *Journal of Agricultural and Food Chemistry*, *58*, 5140–5146.
Shin, J., Simsek, S., Reuhs, B., & Yao, Y. (2008). Glucose release of water-soluble starch-related α-glucans by pancreatin and amyloglucosidase is affected by the abundance of α-1,6 glucosidic linkages. *Journal of Agricultural and Food Chemistry*, *56*, 10879–10886.
Somogyi, M. (1952). Notes on sugar determination. *Journal of Biological Chemistry*, *195*, 19–23.
Thompson, D. B. (2000). On the non-random nature of amylopectin branching. *Carbohydrate Polymers*, *43*, 223–239.
Tomalia, D. A. (2005). Birth of a new macromolecular architecture: Dendrimers as quantized building blocks for nanoscale synthetic polymer chemistry. *Progress in Polymer Science*, *30*, 294–324.
Wong, K., Kubo, A., Jane, J., Harada, K., Satoh, H., & Nakamura, Y. (2003). Structures and properties of amylopectin and phytoglycogen in the endosperm of sugary-1 mutants of rice. *Journal of Cereal Science*, *37*, 139–149.
Yun, S. H., & Matheson, N. K. (1993). Structures of the amylopectins of waxy, normal, Amylase-extender, and wx: Ae genotypes and of the phytoglycogen of maize. *Carbohydrate Research*, *243*, 307–321.
Zeeman, S. C., Umemoto, T., Lue, W. L., Au-Yeyng, P., Martin, C., Smith, A. M., et al. (1998). A mutant of Arabidopsis lacking a chloroplastic isoamylase accumulates both starch and phytoglycogen. *Plant Cell*, *10*, 1699–1711.